

Numerical Contractor Renormalization applied to strongly correlated systems

Sylvain Capponi

Laboratoire de Physique Théorique, CNRS UMR 5152,
Université Paul Sabatier, F-31062 Toulouse, France

(Dated: October 30, 2018)

We demonstrate the utility of effective Hamiltonians for studying strongly correlated systems, such as quantum spin systems. After defining local relevant degrees of freedom, the numerical Contractor Renormalization (CORE) method is applied in two steps: (i) building an effective Hamiltonian with longer ranged interactions up to a certain cut-off using the CORE algorithm and (ii) solving this new model numerically on finite clusters by exact diagonalization and performing finite-size extrapolations to obtain results in the thermodynamic limit. This approach, giving complementary information to analytical treatments of the CORE Hamiltonian, can be used as a semi-quantitative numerical method. For ladder type geometries, we explicitly check the accuracy of the effective models by increasing the range of the effective interactions until reaching convergence. Our results both in the doped and undoped case are in good agreement with previously established results. In two dimensions we consider the plaquette lattice and the *kagomé* lattice as non-trivial test cases for the numerical CORE method. As it becomes more difficult to extend the range of the effective interactions in two dimensions, we propose diagnostic tools (such as the density matrix of the local building block) to ascertain the validity of the basis truncation. On the plaquette lattice we have an excellent description of the system in both the disordered and the ordered phases, thereby showing that the CORE method is able to resolve quantum phase transitions. On the *kagomé* lattice we find that the previously proposed twofold degenerate $S = 1/2$ basis can account for a large number of phenomena of the spin $1/2$ *kagomé* system and gives a good starting point to study the doped case.

PACS numbers: 75.10.Jm, 75.40.Mg, 71.27.+a, 75.50.Ee

I. INTRODUCTION

Low-dimensional quantum magnets are at the heart of current interest in strongly correlated electron systems. These systems are driven by strong correlations and large quantum fluctuations - especially when frustration comes into play - and can exhibit various unconventional phases and quantum phase transitions. Similarly, doping these compounds leads to a rich variety of phases, like superconductivity for instance. One of the major difficulties in trying to understand these systems is that strong correlations often generate highly non trivial low-energy physics. Not only the groundstate of such models is generally not known but also the low-energy degrees of freedom can not be identified easily. Moreover, among the techniques available to investigate these systems, not many have the required level of generality to provide a systematic way to derive low-energy effective Hamiltonians.

Recently the Contractor Renormalization (CORE) method has been introduced by Morningstar and Weinstein¹. The key idea of the approach is to derive an effective Hamiltonian acting on a truncated local basis set, in order to exactly reproduce the low energy spectrum. In principle the method is exact in the low energy subspace, but only at the expense of having *a priori* long-range interactions. The method becomes most useful when one can significantly truncate a local basis set and still restrict oneself to short-range effective interactions. This however depends on the system under consideration and has to be checked systematically. Since its inception the CORE method has been mostly used as an analytical method to study strongly correlated systems^{2,3,4,5}. Some first steps in using the CORE approach and related ideas in a numerical framework have also been undertaken^{6,7,8,9,10}.

The purpose of the present paper is to explore the numerical CORE method as a complementary approach to more analytical CORE procedures (see the contribution by A. Auerbach in this volume), and to discuss its performance in a variety of strongly correlated systems, both frustrated and unfrustrated. The approach consists basically of numerical exact diagonalizations of the effective Hamiltonians. Furthermore we discuss some criteria and tools useful to estimate the quality of the CORE approach. More technical details can be found in related work done in collaboration with D. Poilblanc⁸ and with A. Läuchli and M. Mambrini¹¹.

After reviewing the CORE algorithm, we will present numerical applications to one-dimensional (1D) systems. We will show that the numerical CORE method is able to get rather accurate estimates of physical properties by successively increasing the range of the effective interactions. Then, we discuss two-dimensional (2D) magnetic systems. As in 2D a long ranged cluster expansion of the interactions is difficult to achieve on small clusters, we will discuss some techniques to analyze the quality of the basis truncation. We illustrate these issues on two model systems, the plaquette lattice and the *kagomé* lattice. The plaquette lattice is of particular interest as it exhibits a quantum phase transition from a disordered plaquette state to a long range ordered Néel antiferromagnet, which

cannot be reached by a perturbative approach. We show that a range-two effective model captures many aspects of the physics over the whole range of parameters. The *kagomé* lattice on the other hand is a highly frustrated lattice built of corner-sharing triangles and it is one best-known candidate systems for a spin liquid groundstate. A very peculiar property is the exponentially large number of low-energy singlets in the magnetic gap. We show that already a basic range two CORE approach is able to devise an effective model which exhibits the same exotic low-energy physics.

II. LOW-ENERGY EMERGING DEGREES OF FREEDOM

In various fields, the high-energy description can be well captured by a well-known model, such as the Hubbard or t-J models in the context of high temperature superconductors. However, one is interested in low-energy properties, or similarly long-distance behaviour, which are difficult to compute numerically due to system size limitations.

The spirit of Wilson’s real-space renormalization group¹² is that one can integrate out local degrees of freedom (i.e. high-energy) in order to define new emerging degrees of freedom and derive an effective model which will be valid on larger distances.

The definition of relevant degrees of freedom at a given energy scale is a very deep concept in the sense that one can forget many irrelevant details and derive an effective theory. For instance, chemists know very well that an atom or a molecule are very powerful concepts, even though they do not exist as fundamental particles.

Now, the question is how do we identify the relevant “atoms” and how do we compute an effective theory ? The answer is provided by the CORE algorithm.

A. CORE Algorithm

The CORE method has been proposed by Morningstar and Weinstein in the context of general Hamiltonian lattice models¹. Later Weinstein applied this method with success to various spin chain models². For a review of the method we refer the reader to these original papers and also to a pedagogical article by Altman and Auerbach³ (see also the contribution in this volume by A. Auerbach). Here, we summarize the basic steps before discussing some technical aspects which are relevant in our numerical approach.

CORE Algorithm :

- Choose a small cluster (e.g. rung, plaquette, triangle, etc) and diagonalize it. Keep M suitably chosen low-energy states.
- Diagonalize the full Hamiltonian H on a connected graph consisting of N_c clusters and obtain its low-energy states $|n\rangle$ with energies ε_n .
- The eigenstates $|n\rangle$ are projected on the tensor product space of the states kept and Gram-Schmidt orthonormalized in order to get a basis $|\psi_n\rangle$ of dimension M^{N_c} . As it may happen that some of the eigenstates have zero or very small projection, or vanish after the orthogonalization it might be necessary to explicitly compute more than just the lowest M^{N_c} eigenstates $|n\rangle$.

- Next, the effective Hamiltonian for this graph is built as : $h_{N_c} = \sum_{n=1}^{M^{N_c}} \varepsilon_n |\psi_n\rangle \langle \psi_n|$.

- The connected range- N_c interactions $h_{N_c}^{\text{conn}}$ are determined by subtracting the contributions of all connected subclusters.

- Finally, the effective Hamiltonian is given by a cluster expansion as

$$H^{\text{CORE}} = \sum_i h_i + \sum_{\langle ij \rangle} h_{ij} + \sum_{\langle ijk \rangle} h_{ijk} + \dots$$

This effective Hamiltonian *exactly* reproduces the low-energy physics provided the expansion goes to infinity. However, if the interactions are short-range in the starting Hamiltonian, we can expect that these operators will become smaller and smaller, at least in certain situations. In the following, we will truncate at range r and verify the convergence in several cases. This convergence naturally depends on the number M of low-lying states that are kept on a basic block. By using the reduced density matrix, we will show a way to determine how “good” these states are.

Once an effective Hamiltonian has been obtained, it is still a formidable task to determine its properties. Within the CORE method different routes have been taken in the past. In their pioneering papers, Morningstar and Weinstein have chosen to iteratively apply the CORE method in order to flow to a fixed point that can be analyzed. A different approach has been taken in Refs. [3,4,5] : There the effective Hamiltonian after one or two iterations has been analyzed with mean-field like methods and interesting results have been obtained. Yet another approach - and the one we will pursue in this paper - consists of a single CORE step to obtain the effective Hamiltonian, followed by a numerical simulation thereof. This approach has been explored in a few previous studies^{6,7,8}. The numerical technique we employ is the Exact Diagonalization (ED) method based on the Lanczos algorithm. This technique has easy access to many observables and profits from the symmetries and conservation laws in the problem, i.e. total momentum and the total S^z component.

III. CHAIN AND LADDER GEOMETRIES

In this section, we describe results obtained on $S = 1/2$ spin chain and ladder systems with 2 and 4 legs respectively.

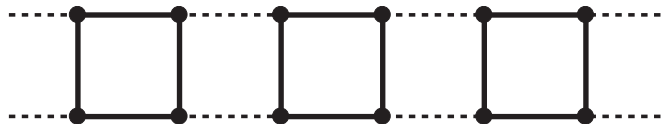


FIG. 1: 2-leg ladder. The basic block used by CORE is a 2×2 plaquette.

In the case of doped systems, we use the isotropic t-J model :

$$\mathcal{H} = J \sum_{i,a} \vec{S}_{i,a} \cdot \vec{S}_{i+1,a} + J \sum_{i,a} \vec{S}_{i,a} \cdot \vec{S}_{i,a+1} - \sum_{i,a} (c_{i,a}^\dagger c_{i+1,a} + h.c.) - \sum_{i,a} (c_{i,a}^\dagger c_{i,a+1} + h.c.)$$

that reduces to the usual Heisenberg hamiltonian in the undoped case, $\mathcal{H} = \sum_{\langle ij \rangle} J \vec{S}_i \cdot \vec{S}_j$, where the exchange constants

J will be limited to nearest neighbours.

We have chosen periodic boundary conditions (PBC) along the chains in order to improve the convergence to the thermodynamic limit.

A. 1D Heisenberg chain

In this simple example, one is able to iterate the CORE procedure in order to obtain the ground-state energy. Let us recall that this model has an exact solution for the ground-state energy $e_0 = -\ln 2 + 1/4$ and has an infinite correlation length so that a numerical approach on a finite system is not obvious. Using CORE and solving up to 12 sites, which is very easy even on a small computer, Weinstein has obtained² a ground-state energy with a relative accuracy of 10^{-5} .

A similar idea consists of increasing the size of the initial block, instead of the range of effective interactions, and this has been applied by Malrieu *et al.* to the same system⁹. Solving numerically up to 22 sites, they have a relative error of 10^{-4} .

Being able to obtain such an accuracy on a ground-state energy by solving small systems compared to the infinite correlation length is very encouraging. Therefore, we have pursued this approach more systematically on other models.

B. Two-leg Heisenberg ladder

The 2-leg Heisenberg ladder has been intensively studied and is known to exhibit a spin gap for all couplings^{13,14,15,16}.

In order to apply our algorithm, we select a 2×2 plaquette as the basic unit (see Fig. 1). The truncated subspace is formed by the singlet ground-state (GS) and the lowest triplet state. Using the same CORE approach, Piekarewicz and Shepard have shown that quantitative results can be obtained within this restricted subspace⁶.

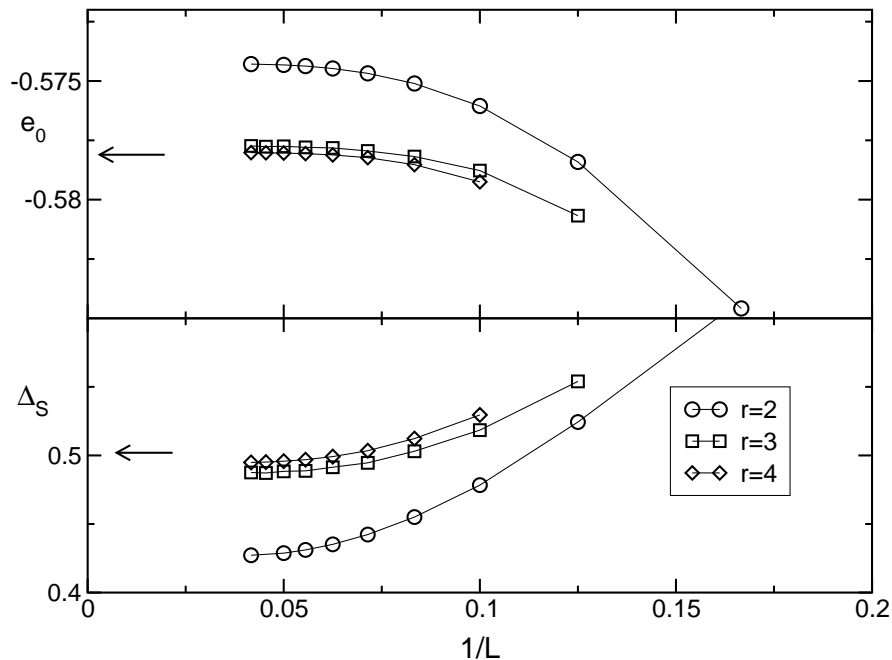


FIG. 2: Ground-state energy per site (e_0) and spin gap (Δ_S) of a $2 \times L$ Heisenberg ladder using CORE method with various range r using PBC. For comparison, we plot the best known extrapolations¹⁴ with arrows.

Since we are dealing with a simple system, we can compute the effective models including rather long-range interactions. It is desirable to compute long-range effective interactions since we wish to check how the truncation affect the physical results and how the convergence is reached.

In a second step, for each of these effective models, we perform a standard Exact Diagonalization (ED) using the Lanczos algorithm on finite clusters up to $N_c = 12$ clusters ($N = 48$ sites for the original model). The GS energy and the spin gap are shown in Fig. 2. The use of PBC allows to considerably reduce finite-size effects since we have an exponential convergence as a function of inverse length. CORE results are in perfect agreement with known results and the successive approximations converge uniformly to the exact results. For instance, the relative errors of range-4 results are 10^{-4} for the GS energy and 10^{-2} for the spin gap. This fast convergence is probably due to the rather short correlation length in an isotropic ladder (typically 3 to 4 lattice spacings¹⁷).

C. Doped case

In order to apply CORE, we choose again a 2×2 plaquette as the basic block. In addition to the magnetic states, we decide to keep the lowest 2-hole state. Therefore, the effective degrees of freedom are hard-core bosons (triplets and hole pairs). A similar approach has been used to study the 2-dimensional case^{3,18}.

In Ref. [8], we have shown that this effective bosonic model reproduces many features of the doped 2-leg ladder such as the persistence of the spin gap, the existence of a triplet-hole pair bound state, as well as the characteristic exponent of the superconducting correlations. A similar model had been proposed previously¹⁹, but the parameters were obtained from DMRG data obtained on large systems. Here, we can deduce the effective parameters by using CORE method, i.e. by solving small clusters.

Following a similar approach, we have also studied the 4-leg t-J ladder⁸. Qualitatively, the physics is very similar to the 2-leg case, albeit with smaller energy scales. In Fig. 3, we draw density-density correlations obtained with the bosonic effective model for various dopings. Upon increasing doping, we observe a clear tendency of the hole pairs to align along the diagonal $(1, \pm 1)$ directions (for doping larger than $1/8$) with a periodicity corresponding to one pair every two plaquettes, a behavior also reported in DMRG calculations^{20,21} and reminiscent of the picture of diagonal stripes. In our case, PBC were used in the leg direction so that stripes formation is intrinsic and not due to any boundary effects.

Therefore, with CORE method, we have both the advantage of working in a reduced subspace and not being limited to the perturbative regime. Amazingly, we have observed that for a very small effort (solving a small cluster), the effective Hamiltonian gives much better results than perturbation theory. It also gives an easier framework to

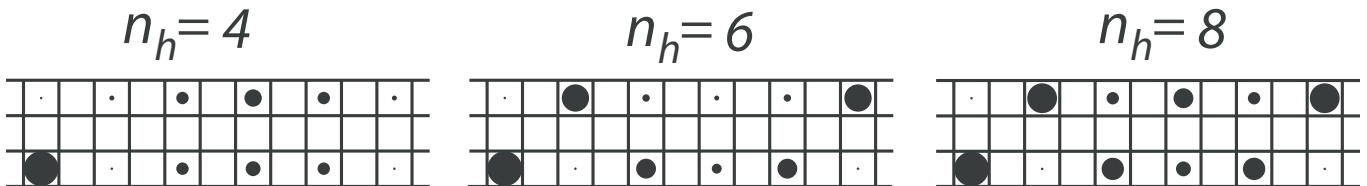


FIG. 3: Hole-pair density-density correlation on a 4×12 ladder at $J/t = 0.35$ for different number of holes n_h . Correlations are measured from the reference plaquette on the lower left corner. The surfaces of the dots are proportional to the values of the correlations.

systematically improve the accuracy by including longer range interactions.

For these models, the good convergence of CORE results may be due to the fact that the GS in the isotropic limit is adiabatically connected to the perturbative one. In the following part we will therefore study 2D models where a quantum phase transition occurs as one goes from the perturbative to the isotropic regime.

IV. TWO DIMENSIONAL SPIN MODELS

In this section we would like to discuss the application of the numerical CORE method to two dimensional quantum spin systems. We will present spectra and observables and also discuss a novel diagnostic tool - the density matrix of local objects - in order to justify the truncation of the local state set.

One major problem in two dimension is the more elaborate cluster expansion appearing in the CORE procedure. We therefore try to keep the range of the interactions minimal, but we still demand a reasonable description of low energy properties of the system. We will therefore discuss some ways to detect under what circumstances the short-range approximations fail and why.

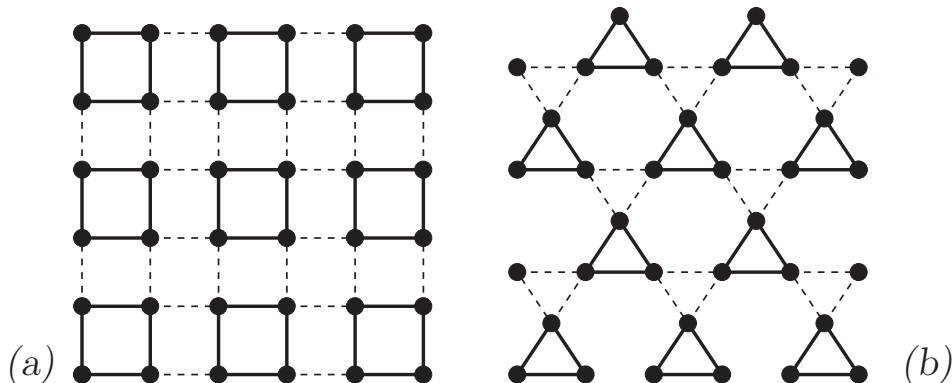


FIG. 4: (a) The plaquette lattice. Full lines denote the plaquette bonds J , dashed lines denote the inter-plaquette coupling J' . (b) The trimerized *kagomé* lattice. Full lines denote the up-triangle J bonds, dashed lines denote the down-triangle coupling J' . The standard *kagomé* lattice is recovered for $J'/J = 1$.

As a first example we discuss the plaquette lattice [Fig. 4 (a)], which exhibits a quantum phase transition from a gapped plaquette-singlet state with only short ranged order to a long range ordered antiferromagnetic state as a function of the interplaquette coupling^{22,23,24,25}. We will show that the CORE method works particularly well for this model by presenting results for the excitation spectra and the order parameter. It is also a nice example of an application where the CORE method is able to correctly describe a quantum phase transition, thus going beyond a perturbation scheme.

The second test case is the highly frustrated *kagomé* lattice [Fig. 4 (b)] which has been intensively studied for $S = 1/2$ during the last few years^{26,27,28,29,30}. Its properties are still not entirely understood, but some of the features are well accepted by now: There is no simple local order parameter detectable, neither spin order nor valence bond crystal order. There is probably a small spin gap present and most strikingly an exponentially growing number of low-energy singlets emerges below the spin gap. We will discuss a convenient CORE basis truncation which has emerged from a perturbative point of view^{29,31,32}.

A. Plaquette lattice

The CORE approach starts by choosing a suitable decomposition of the lattice and a subsequent local basis truncation. In the plaquette lattice the natural decomposition is directly given by the uncoupled plaquettes. Among the 16 states of an isolated plaquette we retain the lowest singlet [$K = (0, 0)$] and the lowest triplet [$K = (\pi, \pi)$]. The standard argument for keeping these states relies on the fact that they are the lowest energy states in the spectrum of an isolated plaquette.

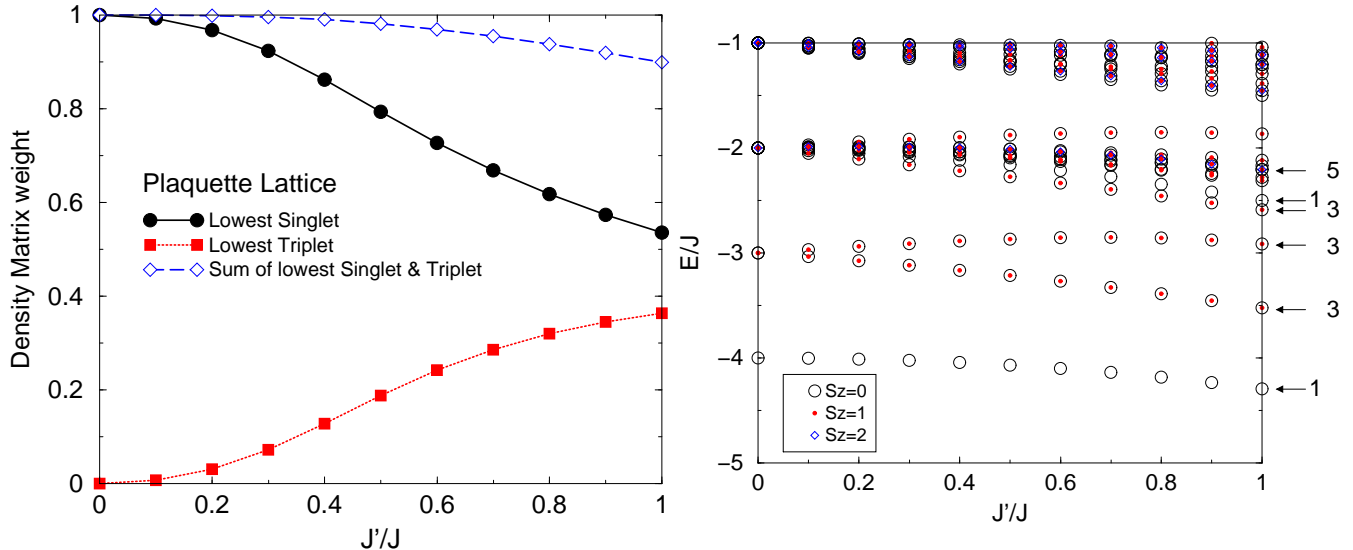


FIG. 5: (a) Left panel : Density matrix weights of the two most important states on a strong (J -bonds) plaquette as a function of J'/J . These results were obtained by ED with the original Hamiltonian on a 4×4 cluster. (b) Right panel : Low-energy spectrum of two coupled plaquettes. The states targeted by the CORE algorithm are indicated by arrows together with their $SU(2)$ degeneracy.

As discussed in Ref. [11], the density matrix of a plaquette in the fully interacting system gives clear indications whether the basis is suitably chosen. In Fig. 5(a) we show the evolution of the density matrix weights of the lowest singlet and triplet as a function of the interplaquette coupling. Even though the individual weights change significantly, the sum of both contributions remains above 90% for all $J'/J \leq 1$. We therefore consider this a suitable choice for a successful CORE application.

A next control step consists in calculating the spectrum of two coupled plaquettes, and one monitors which states are targeted by the CORE algorithm. We show this spectrum in Fig. 5(b) along with the targeted states. We realize that the 16 states of our tensor product basis cover almost all the low energy levels of the coupled system. There are only two triplets just below the $S = 2$ multiplet which are missed.

In order to locate the quantum phase transition from the paramagnetic, gapped regime to the Néel ordered phase, a simple way to determine the onset of long range order is desirable. We chose to directly couple the order parameter to the Hamiltonian and to calculate generalized susceptibilities by deriving the energy with respect to the external coupling. Its simplicity relies on the fact that only eigenvalues are necessary. Similar approaches have been used so far in ED and QMC calculations^{33,34}.

Our results in Fig. 6 show the evolution of the staggered moment per site in a rescaled external staggered field for different inter-plaquette couplings J' and different system sizes (up to 8×8 lattices). We note the appearance of an approximate crossing of the curves for different system sizes, once Néel LRO sets in. This approximate crossing relies on the fact that the slope of the staggered moment diverges at least linearly in N in the ordered phase³⁴. We then consider this crossing feature as an indication of the phase transition and obtain a value of the critical point $J_c/J = 0.55 \pm 0.05$. This estimate is in good agreement with previous studies using various methods^{22,23,24,25}.

It is well known that the square lattice ($J'/J = 1$) is Néel ordered. One possibility to detect this order in ED is to calculate the so-called *tower of excitation*, i.e. the complete spectrum as a function of $S(S+1)$, S being the total spin of an energy level³⁵. In the case of standard collinear Néel order a prominent feature is an alignment of the lowest level for each S on a straight line, forming a so called “Quasi-Degenerate Joint States” (QDJS) ensemble³⁶, which is clearly separated from the rest of the spectrum on a finite size sample. We have calculated the tower of states within the CORE approach (Fig. 7). Due to the truncated Hilbert space we cannot expect to recover the entire

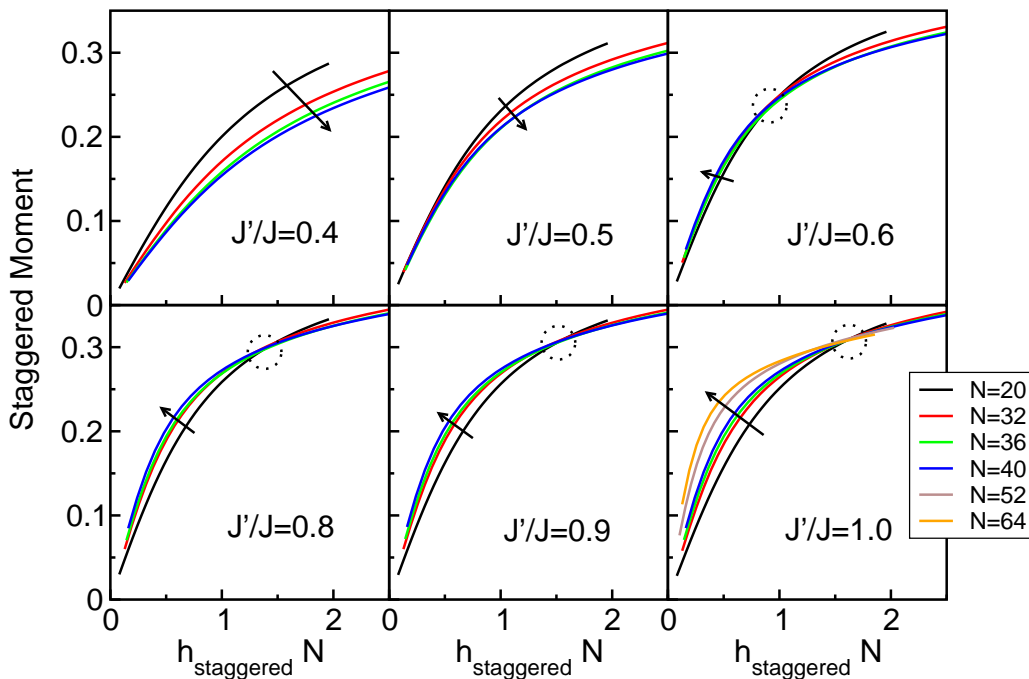


FIG. 6: Staggered moment per site as a function of the rescaled applied staggered field for the plaquette lattice and different values of J'/J . Circles denote the approximate crossing point of curves for different system sizes. We take the existence of this crossing as a phenomenological indication for the presence of Néel LRO. In this way the phase transition is detected between $0.5 < J'_c/J < 0.6$, consistent with previous estimates. The arrows indicate curves for increasing system sizes: 20, 32, 36, 40 and also 52, 64 for the isotropic case.

spectrum. Surprisingly however the CORE tower of states successfully reproduces the general features observed in ED calculations of the same model³⁷: (a) a set of QDJS with the correct degeneracy and quantum numbers (in the folded Brillouin zone); (b) a reduced number of magnon states at intermediate energies, both set of states rather well separated from the high energy part of the spectrum.

B. *kagomé* systems with half-integer spins

In the past 10 years many efforts have been devoted to understand the low energy physics of the *kagomé* antiferromagnet (KAF) for spins $1/2$ ^{26,27,28,29,30}. At the theoretical level, the main motivation comes from the fact that this model is the only known example of a two-dimensional Heisenberg spin liquid. Even though many questions remain open, some very exciting low-energy properties of this system have emerged. Let us summarize them briefly: (i) the GS is a singlet ($S = 0$) and has no magnetic order. Moreover no kind of more exotic ordering (dimer-dimer, chiral order, etc.) have been detected using unbiased methods; (ii) the first magnetic excitation is a triplet ($S = 1$) separated from the GS by a rather small gap of order $J/20$; (iii) more surprisingly the spectrum appears as a continuum of states in all spin sectors. In particular the spin gap is filled with an exponential number of singlet excitations: $\mathcal{N}_{\text{singlets}} \sim 1.15^N$; (iv) the singlet sector of the KAF can be very well reproduced by a short-range resonating valence bond approach involving only nearest-neighbor dimers.

From this point of view, the spin $1/2$ KAF with its highly unconventional low-energy physics appears to be a very sharp test of the CORE method and it was also recently studied in Ref. [5]. The case of higher half-integer spins $S = 3/2, 5/2 \dots$ KAF is also of particular interest, since it is covered by approximative experimental realizations³⁸.

In this section we discuss in detail the range-two CORE Hamiltonians for spin $1/2$ KAF considered as a set of elementary up-triangles with couplings J , coupled by down-triangles with couplings J' [see Fig. 4 (b)].

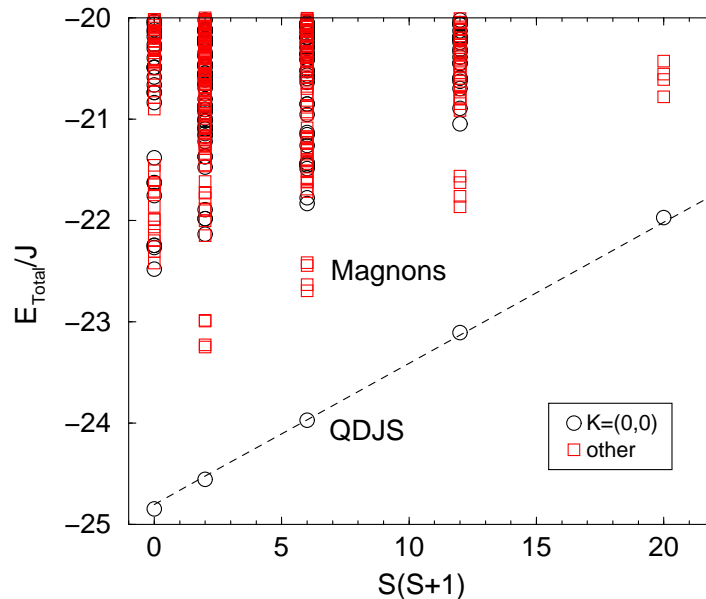


FIG. 7: Tower of states obtained with a range-2 CORE Hamiltonian on an effective $N = 36$ square lattice (9-site CORE cluster) in different reduced momentum sectors. The tower of states is clearly separated from the decimated magnons and the rest of the spectrum.

1. Choice of the CORE basis

We decide to keep the two degenerate $S = 1/2$ doublets on a triangle for the CORE basis. In analogy with the the plaquette lattice we calculate the density matrix of a single triangle embedded in a 12 site *kagomé* lattice, in order to get information on the quality of the truncated basis. The results show that the targeted states exhaust 95%, which indicates that the approximation seems to work particularly well, thereby providing independent support for the adequacy of the basis chosen in a related mean-field study²⁹.

We continue the analysis of the CORE basis by monitoring the evolution of the spectra of two coupled triangles in the *kagomé* geometry as a function of the inter-triangle coupling J' , as well as the states selected by the range-two CORE algorithm. The spectrum is shown in Fig. 8. We note the presence of a clear gap between the 16 lowest states – correctly targeted by the CORE algorithm – and the higher lying bands. This can be considered an ideal case for the CORE method. Based on this and the results of the density matrix we expect the CORE range-two approximation to work quite well.

2. Simulations for $S = 1/2$

We now focus on the effective model describing the standard *kagomé* lattice, and we present several distinct physical properties, such as the tower of excitations, the evolution of the triplet gap as a function of system size and the scaling of the number of singlets in the gap. These quantities have been discussed in great detail in previous studies of the *kagomé* $S = 1/2$ antiferromagnet^{26,27,28,29,30}.

First we calculate the tower of excitations for a *kagomé* $S = 1/2$ system on a 27 sites sample. The data is plotted in Fig. 9. The structure of the spectrum follows the exact data of Ref. [27] rather closely; i.e there is no QDJS ensemble visible, a large number of $S = 1/2$ states covering all momenta are found below the first $S = 3/2$ excitations and the spectrum is roughly bounded from below by a straight line in $S(S + 1)$. Note that the tower of states we obtain here is strikingly different from the one obtained in the Néel ordered square lattice case, see Fig. 7.

Next we calculate the spin gap using the range-two and three (containing a closed loop of triangles) CORE Hamiltonians. We have a reasonable agreement with ED results when available but there are strong finite size effects. The precision of the CORE gap data is not accurate enough to make a reasonable prediction on the spin gap in the thermodynamic limit. However we think that the CORE data are compatible with a finite spin gap.

Finally we determine the number of nonmagnetic excitations within the magnetic gap for a variety of system sizes up to 39 sites. Similar studies of this quantity in ED gave evidence for an exponentially increasing number of singlets

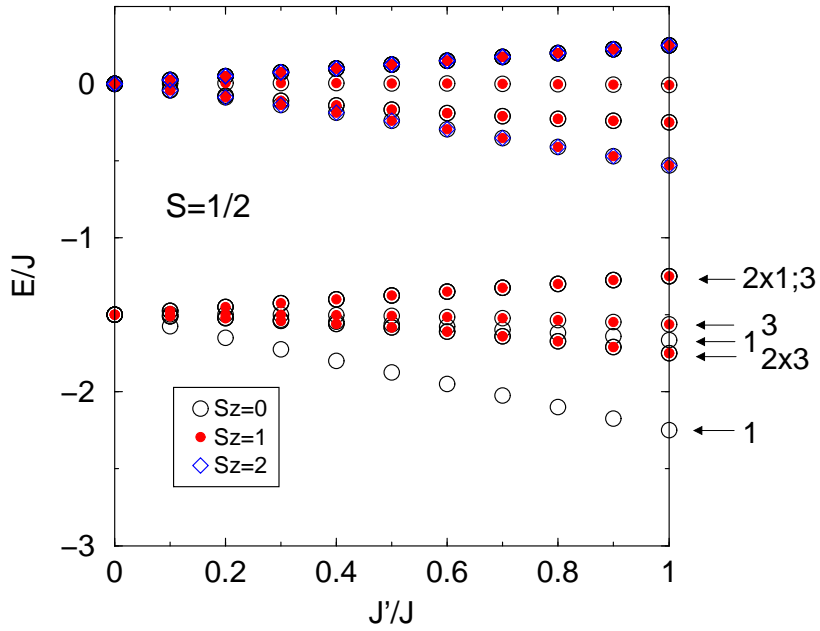


FIG. 8: Spectrum of two coupled triangles in the *kagomé* geometry with $S = 1/2$ spins. The entire lowest band containing 16 states is successfully targeted by the CORE algorithm.

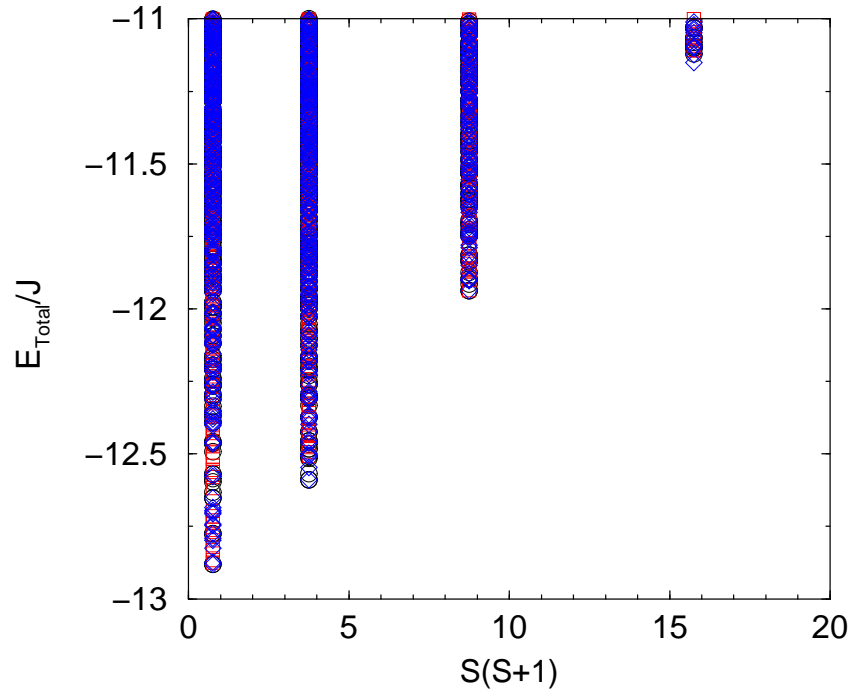


FIG. 9: Tower of states obtained with a range-two CORE Hamiltonian on an effective $N = 27$ *kagomé* lattice (9-site CORE cluster). There is a large number of low-lying states in each S sector. The symbols correspond to different momenta.

in the gap^{27,28}. We display our data in comparison to the exact results in Fig. 10. While the precise numbers are not expected to be recovered, the general trend is well described with the CORE results. For both even and odd N samples we see an exponential increase of the number of these nonmagnetic states. In the case of $N = 39$ for example, we find 506 states below the first magnetic excitation.

These results emphasize the validity of the two doublet basis for the CORE approach on the *kagomé* spin $1/2$

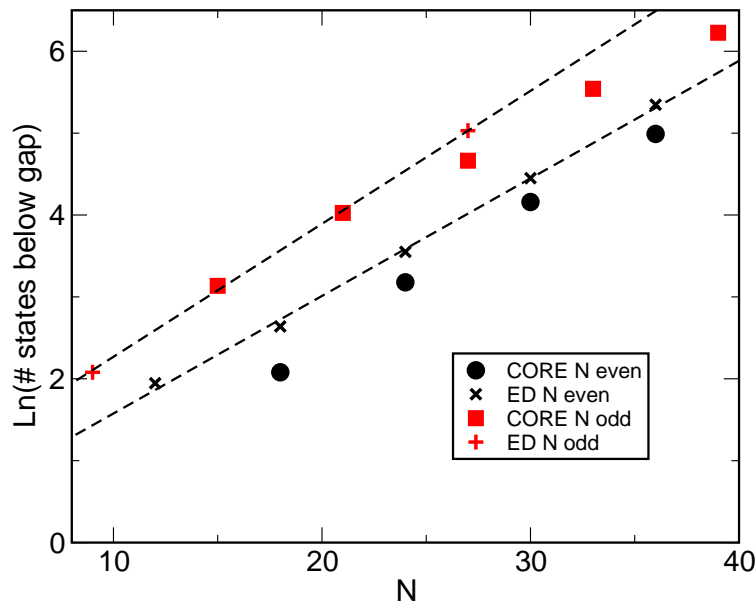


FIG. 10: Logarithm of the number of states within the magnetic gap. Results obtained with the CORE range-two Hamiltonian. For comparison exact data obtained in Refs. [27,28] are shown. The dashed lines are linear fits to the exact diagonalization data.

system.

It also gives an easier starting point to study the effect of doping a short-range Resonating Valence Bond state. Using CORE and other techniques, we have shown that the doped *kagomé* lattice at 1/3-doping undergoes a Peierls transition towards a “Valence Bond Solid”³⁹. This instability is due only to electronic correlations and gives an example of a 2D Bond Order Wave. It illustrates how doped antiferromagnets on highly frustrated lattices can partially avoid frustration by lowering the lattice symmetry.

V. CONCLUSIONS

We have discussed the usefulness of real-space renormalization techniques - the so-called numerical Contractor Renormalization (CORE) method - in obtaining local low-energy relevant degrees of freedom and an effective theory in the context of low-dimensional strongly correlated systems. This method consists of two steps: (i) building an effective Hamiltonian acting on the low-energy degrees of freedom of some elementary block; and (ii) studying this new model numerically on finite-size clusters, using a standard Exact Diagonalization or similar approach.

Like in other real-space renormalization techniques, the effective model usually contains longer range interactions. The numerical CORE procedure will be most efficient provided the effective interactions decay sufficiently fast. We discussed the validity of this assumption in several cases.

For ladder type geometries, we explicitly checked the accuracy of the effective models by increasing the range of the effective interactions until reaching convergence. Our results on doped and undoped ladders are in good agreement with previously established results.

In two dimensions, we have used the density matrix as a tool to check whether the restricted basis gives a good enough representation of the exact states. When this is the case, as for the plaquette lattice or the $S = 1/2$ *kagomé* lattice, the lowest order range-two effective Hamiltonian gives semi-quantitative results, even away from any perturbative regime. For example we can successfully describe the plaquette lattice, starting from the decoupled plaquette limit through the quantum phase transition to the Néel ordered state at isotropic coupling. Furthermore we can also reproduce many aspects of the exotic low-energy physics of the $S = 1/2$ *kagomé* lattice.

Therefore within the CORE method, we can have both the advantage of working in a strongly reduced subspace and not being limited to the perturbative regime.

We thus believe that the numerical CORE method can be used systematically to explore possible ways of generating low-energy effective Hamiltonians starting from strongly correlated models.

Acknowledgments

I thank A. Läuchli, M. Mambrini and D. Poilblanc for their contributions to this work. I also thank A. Auerbach for introducing me to the CORE algorithm and for many insightful discussions. Finally, I acknowledge fruitful discussions with F. Alet, J.-P. Malrieu and F. Mila.

-
- ¹ C. J. Morningstar, and M. Weinstein, *Phys. Rev. D*, **54**, 4131 (1996).
² M. Weinstein, *Phys. Rev. B*, **6317**, 174421 (2001).
³ E. Altman, and A. Auerbach, *Phys. Rev. B*, **65**, 104508 (2002).
⁴ E. Berg, E. Altman, and A. Auerbach, *Phys. Rev. Lett.*, **90**, 147204 (2003).
⁵ R. Budnik, and A. Auerbach, *Phys. Rev. Lett.*, **93**, 187205 (2004).
⁶ J. Piekarewicz, and J. R. Shepard, *Phys. Rev. B*, **56**, 5366 (1997).
⁷ J. Piekarewicz, and J. R. Shepard, *Phys. Rev. B*, **57**, 10260 (1998).
⁸ S. Capponi, and D. Poilblanc, *Phys. Rev. B*, **66**, 180503 (2002).
⁹ J. P. Malrieu, and N. Guihéry, *Phys. Rev. B*, **6308**, 085110 (2001).
¹⁰ M. Al Hajj, N. Guihéry, J. P. Malrieu, and P. Wind, *Phys. Rev. B*, **70**, 094415 (2004).
¹¹ S. Capponi, A. Läuchli, and M. Mambrini, *Phys. Rev. B*, **70**, 104424 (2004).
¹² K. G. Wilson, *Rev. Mod. Phys.*, **47**, 773 (1975).
¹³ T. Barnes, E. Dagotto, J. Riera, and E. S. Swanson, *Phys. Rev. B*, **47**, 3196 (1993).
¹⁴ S. R. White, R. M. Noack, and D. J. Scalapino, *Phys. Rev. Lett.*, **73**, 886 (1994).
¹⁵ B. Frischmuth, B. Ammon, and M. Troyer, *Phys. Rev. B*, **54**, R3714 (1996).
¹⁶ E. Dagotto, and T. M. Rice, *Science*, **271**, 618 (1996).
¹⁷ M. Greven, R. J. Birgeneau, and U. J. Wiese, *Phys. Rev. Lett.*, **77**, 1865 (1996).
¹⁸ H. D. Chen, S. Capponi, F. Alet and S. C. Zhang, *Phys. Rev. B*, **70**, 024516 (2004). See also the contribution in this volume by S. C. Zhang.
¹⁹ T. Siller, M. Troyer, T. M. Rice and S. R. White, *Phys. Rev. B*, **63**, 195106 (1996).
²⁰ S. R. White, and D. J. Scalapino, *Phys. Rev. B*, **55**, 14701 (1997).
²¹ T. Siller, M. Troyer, T. M. Rice, and S. R. White, *Phys. Rev. B*, **65**, 205109 (2002).
²² A. Koga, S. Kumada, and N. Kawakami, *J. Phys. Soc. Jpn.*, **68**, 2373 (1999).
²³ A. Koga, S. Kumada, and N. Kawakami, *J. Phys. Soc. Jpn.*, **68**, 642 (1999).
²⁴ A. Läuchli, S. Wessel, and M. Sigrüst, *Phys. Rev. B*, **66**, 014401 (2002).
²⁵ A. Voigt, *Computer Physics Communications*, **146**, 125 (2002).
²⁶ P. W. Leung, and V. Elser, *Phys. Rev. B*, **47**, 5459 (1993).
²⁷ P. Lecheminant, B. Bernu, C. Lhuillier, L. Pierre, and P. Sindzingre, *Phys. Rev. B*, **56**, 2521 (1997).
²⁸ C. Waldtmann, H. Everts, B. Bernu, C. Lhuillier, P. Sindzingre, P. Lecheminant, and L. Pierre, *Eur. Phys. J. B*, **2**, 501 (1998).
²⁹ F. Mila, *Phys. Rev. Lett.*, **81**, 2356 (1998).
³⁰ M. Mambrini, and F. Mila, *Eur. Phys. J. B*, **17**, 651 (2000).
³¹ V. Subrahmanyam, *Phys. Rev. B*, **52**, 1133 (1995).
³² C. Raghun, I. Rudra, S. Ramasesha, and D. Sen, *Phys. Rev. B*, **62**, 9484 (2000).
³³ M. Calandra, and S. Sorella, *Phys. Rev. B*, **61**, 11894–11897 (2000).
³⁴ L. Capriotti, *Int. J. Mod. Phys. B*, **15**, 1799 (2001).
³⁵ P. W. Anderson, *Phys. Rev.*, **86**, 694 (1952).
³⁶ B. Bernu, C. Lhuillier, and L. Pierre, *Phys. Rev. Lett.*, **69**, 2590 (1992).
³⁷ P. Sindzingre, C. Lhuillier, and J. B. Fouet, *Int. J. Mod. Phys. B*, **17**, 5031 (2003).
³⁸ L. Limot, P. Mendels, G. Collin, C. Mondelli, B. Ouladdiaf, H. Mutka, N. Blanchard, and M. Mekata, *Phys. Rev. B*, **65**, 144447 (2002).
³⁹ M. Indergand, A. Läuchli, S. Capponi and M. Sigrüst, in preparation.